

# BROADBAND IMPEDANCE OF THE B FACTORY.

S. Heifets  
 Stanford Linear Accelerator Center  
 Stanford University, Stanford, CA 94309 USA

## Abstract

The broadband impedance is described phenomenologically by expansion over  $\sqrt{\omega}$ . It is shown that different terms of the expansion correctly describe particular impedance-generating elements. The broadband impedance and the wake function of the B factory [1] are reconstructed with numeric code TBCI. The losses at the interaction region due to excitation of the higher order modes (HOM) are estimated.

## I. INTRODUCTION

Impedance can be constructed as a sum of narrow- and broad-band impedances. The narrow-band impedance is typical for the rf cavities and described in the modal analysis as the sum

$$Z(\omega) = i \sum \chi_l \left( \frac{1}{\omega - \omega_l + i\gamma_l} + \frac{1}{\omega + \omega_l + i\gamma_l} \right), \quad (1)$$

where  $\chi_l$  and  $\omega_l$  are the loss factor and the frequency of the  $l$ th mode and the width  $\gamma_l = \omega_l/2Q_l$ .

Broadband impedance often has been described empirically as the impedance of a single low-Q mode, but this is no more than data fitting, and has no other justification. Here, we further develop the approach used by K. Bane in his analysis of the impedance of the SLC damping ring [2].

Broadband impedance may be represented in the form of the expansion over  $\sqrt{\omega}$  (we imply the time dependence  $\exp\{-i\omega t\}$ ):

$$Z(\omega) = -i\omega L + R_\Omega + (1-i)\sqrt{\omega}B + (1+i)Z_C\sqrt{\omega_0/\omega} + \dots \quad (2)$$

The coefficients  $L, R, B, Z_C \dots$  are real, as they follow from the analytic property of the impedance.

The first term represents inductive impedance. This behavior of the impedance at low frequencies also can be expected from Eq. (1) in the limit  $\omega \rightarrow 0$ , giving  $L = -i\omega \sum (\chi_l/\omega_l^2)$ . Impedance remains inductive for small discontinuities at rather high frequencies.

The second term in the expansion (2) is the low-frequency resistive impedance; the third term has the structure of the impedance of the resistive walls; and the last term describes the high-frequency tail of the impedance of the rf cavities. At high frequencies, the narrow-band impedance rolls off as  $\omega^2$ , and is small compared to the high-frequency tail,

$$\frac{Z(n)}{n} = (1+i) \frac{Z_{cav}}{n^{3/2}}.$$

At the bunch frequencies  $\omega/c \simeq 1/\sigma$ , this is very close to the SPEAR scaling

$$Z/n \propto \left(\frac{\sigma}{b}\right)^{1.68}, \quad (3)$$

where  $b$  is assumed to be equal to the beam-pipe radius.

\*Work supported by Department of Energy contract DE-AC03-76SF00515.

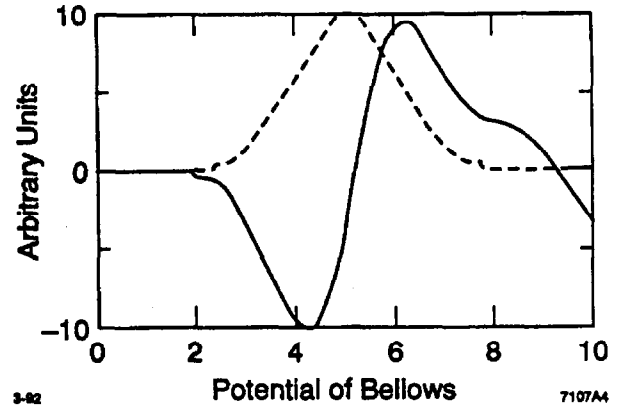


Figure 1. The wake potential of a bellow, as given by TBCI. The wake is typical for the discontinuities, giving inductive impedance.

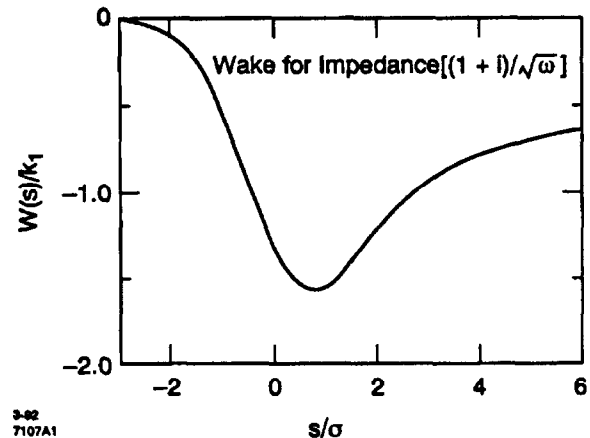


Figure 2. Wake  $W(s)$  in units  $\chi/(V/pC)$  for the model impedance.

Simulations show that, for the B factory, it is sufficient to describe the impedance by three parameters: inductance  $L$ , resistivity  $R_\Omega$ , and the parameter  $Z_C$ . The wake function for these cases is quite different, being proportional to the bunch density  $\rho$   $W(s) = 4\pi(R_\Omega/Z_0)\rho(s)$  for constant  $Z(\omega) = R_\Omega$ , and to the derivative  $W(s) = L(\partial\rho(s)/\partial s)$  for the inductive impedance [see Fig. 1]. The wake function in the last case has maximum and minimum at  $s = \pm\sigma$ :

$$W_{\max} = -W_{\min} = \frac{L}{\sqrt{2\pi e} \sigma^2}, \quad (4)$$

and the loss factor is zero. The dependence  $W(s)$  for the last term in (2) [see Fig. 2] is quite similar to the behavior of the wake of the rf cavity given by TBCI [see Fig. 3].

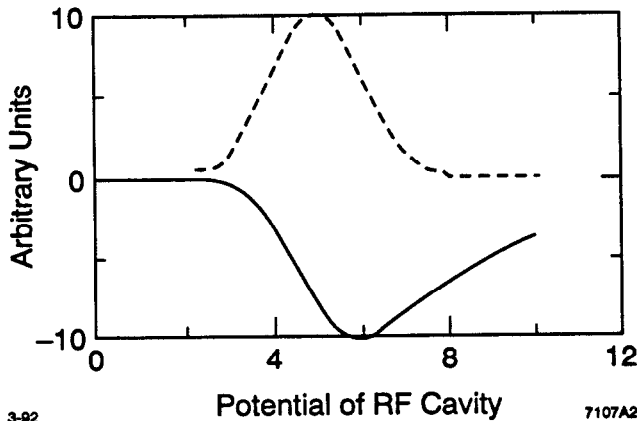


Figure 3. Wake  $W(s)$  of the re-entrant rf cavity, given by TBCI.

In the following, we assume  $R = 350$  m and  $\sigma = 1$  cm.

## II. IMPEDANCE GENERATING ELEMENTS

The main sources of the impedance are 20 re-entrant rf cavities. The rest comes from any variations of the cross-section of the beam pipe in the ring. Impedance-generating elements per 1/12 of the ring (12 cells of an arc and a straight section) are summarized in Table 1 (rf cavities, a feedback system, injection system, collimators, and the interaction region (IR) have to be taken into account, in addition to the elements given in the table). Some elements (for example, diagnostics) certainly will be added later. More details of the vacuum chamber may be found in the Conceptual Design Report (CDR) [1].

Table 1  
Average number of the impedance-generating elements in 1/12 of the ring

Flanges	60
BPM	12
Vacuum ports	24
Bellows	12
Clearing electrodes	4
Valve	1
Taper	1
Slots of the distributed pumps	$3.0 \times 10^3$ .

The parameter  $Z_C$  has been found from the known loss-factors of the low-frequency modes and the total loss factor given by TBCI for the re-entrant rf cavity. Resistive-wall impedance was found as the average over the copper elliptical pipe in the arcs and the round stainless steel pipe in the straight sections. The impedance of inductive elements were calculated using TBCI, Kurrenoy's formula for slots [3], and the analytic formula for shallow transitions,

$$L = 2g \frac{b-a}{a}.$$

Kickers for the feedback system and four-button BPMs were described using results of measurements [4]. The IR API-

ARY7.5E, generated by M. Sullivan, is a 3-dimensional structure with a number of tapers asymmetrically placed in the horizontal and vertical planes. The impedance was estimated using TBCI with proper azimuthal averaging. The wake field found by TBCI corresponds to the inductive impedance with  $Z(n)/n = 1.8 \times 10^{-3} \Omega$ , or  $L = 2$  nH. The real part is small:  $\text{Re}Z/n = 12.5 \Omega$ . The total power deposition in the IR by two beams is

$$P_{\text{tot}} = e \langle \chi \rangle (I_{\text{avg}}^+ N_B^+ + I_{\text{avg}}^- N_{\text{avg}}^-)$$

with the averaged currents specified in the CDR,  $P_{\text{tot}} = 1.77$  KW. The contribution from the low-energy beam is about two times the contribution of the high-energy beam. This is very small compared to the power deposited by the synchrotron radiation (about 94 kW, M. Sullivan [1]).

The Ohmic losses are much smaller. The power deposition per unit length by a beam with  $n_B$  bunches in the ring is

$$\frac{dP}{dz} = n_B f_{\text{rev}} \left( \frac{e^2}{2\pi b} \right) \frac{N_B^2}{\sigma_b^{3/2}} \sqrt{\frac{2}{\sigma Z_0}} \Gamma \left( \frac{3}{4} \right).$$

For a beryllium pipe,  $\sigma = 3.1 \times 10^5 \Omega^{-1} \text{cm}^{-1}$ ,  $b = 2.5$  cm, that gives 0.86 W/cm for two bunches with CDR parameters  $n_B = 1658$ ,  $f_{\text{rev}} = 136$  KHz,  $N_B = (4.08 \text{ and } 5.91 \cdot 10^{10})$ . The power deposited in HOM will be absorbed mostly outside of the IR. The waves generated outside of the IR and absorbed within IR deposit very little energy, because the average loss factor per unit length outside of the IR (excluding rf cavities) is much smaller than that of the IR. Energy deposition could be enhanced substantially if there were trapped modes in the IR, provided their wave length is a multiple of the bunch spacing. We tried to find the trapped modes in the structure which reproduces the real structure within  $\pm 25$  cm from the IP and then is continued with the straight pipes. The MAFIA code (Kwok Ko simulations) failed to find trapped modes, although a single mode resembles such a mode [see Fig. 4]. This is not surprising in an open structure such as APIARY7.5E.



Figure 4. A candidate for a trapped mode at the IR; MAFIA output (Kwok Ko).

The total impedance is

$$Z(\omega) = -in \text{Im} \left( \frac{Z}{n} \right) + R_\Omega + 2.55 (1 - i) \sqrt{n} + 5.55 \cdot 10^3 \frac{1+i}{\sqrt{n}} (\Omega).$$

The real part [see Fig. 5] is dominated by rf cavities and the stainless steel resistive walls. The rest of the ring gives a small contribution that can be described as a constant resistive impedance  $R_\Omega = 117 \Omega$  given by bellows ( $75 \Omega$ ), tapers ( $29.5 \Omega$ ), and IR ( $12.5 \Omega$ ).

The contributions to the inductive part of the parameter  $\text{Im}(Z(n)/n)$  are given in Table 2.

With the contingency  $Z(n)/n = 0.03 \Omega$  for the injection system and collimators, the total inductive impedance is  $Z(n)/n = 0.10 \Omega$ .

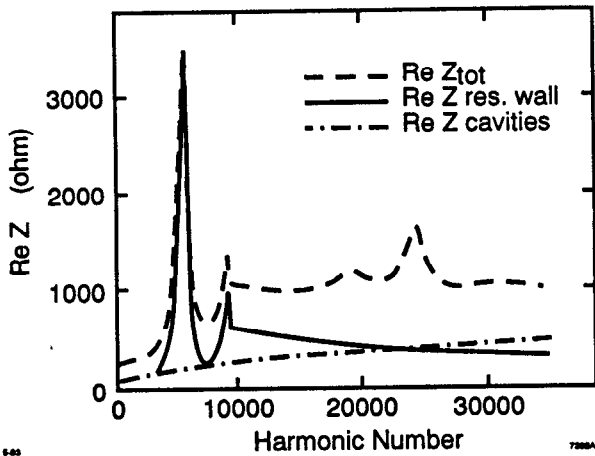


Figure 5. The real part of the longitudinal impedance.

BPMs	$0.13 \times 10^{-4}$
Vacuum ports	$0.5 \times 10^{-4}$
Bellows	$0.62 \times 10^{-2}$
Flanges	0.001
Valves	0.006
Taper	0.016
DIP screen	0.030
Feedback system	0.0035
Interaction region	0.002
Injection crotches	$3.6 \times 10^{-3}$
Total	<u>0.07</u>

The wake function is shown in Fig. 6. Figure 7 gives the partial contribution to the total wake from the impedances of resistive walls and the cavity, and correspondingly, the inductive and real parts of the impedance generated by discontinuities, from the Table 2.

### ACKNOWLEDGMENTS

I am very thankful to Kwok Ko for simulations with MAFIA, and to K. Bane for useful discussions.

### REFERENCES

- [1] "An Asymmetric B Factory, Conceptual Design Report," BL PUB-5303, SLAC-372 (1991).

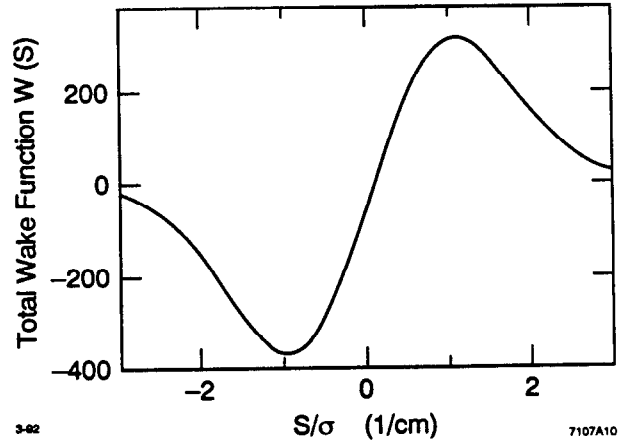


Figure 6. The total wake function.

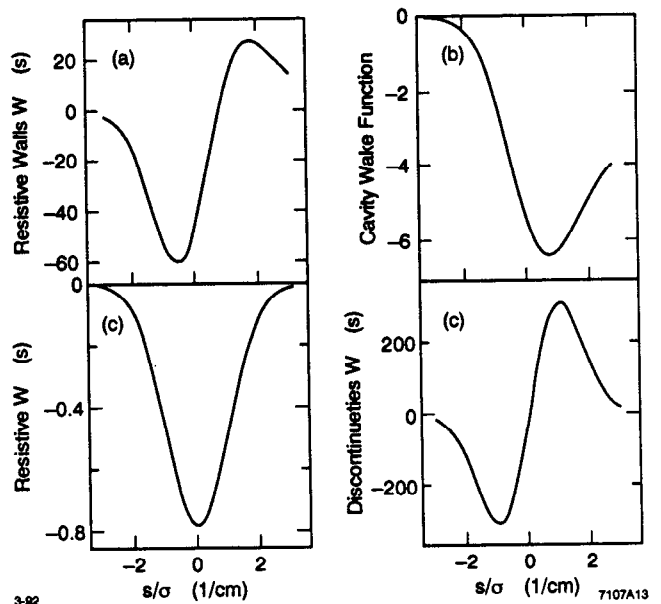


Figure 7. Partial contribution to the total wake from the impedances of (a) resistive walls, (b) cavity, (c) inductive, and (d) real parts of the impedance generated by discontinuities, correspondingly.

- [2] K. Bane, "The Calculated Longitudinal Impedance of the SLC Damping Ring, SLAC-PUB-4618 (1988).  
 [3] S. S. Kurennoy, "On the Coupling Impedance of a Hole or Slot," CERN-SL/91-29 (AP) (1991).  
 [4] A. Jacob and G. R. Lambertson, "Impedance Measurements on Button Electrodes," E-4, LSAP-46, LBL-25955.